Biochemistry and Biophysics Reports 2 (2015) 94–102

Contents lists available at ScienceDirect

Biochemistry and Biophysics Reports

journal homepage: www.elsevier.com/locate/bbrep

HaCaT anchorage blockade leads to oxidative stress, DNA damage and DNA methylation changes

Rodrigo A. da Silva *, Flavia Sammartino Mariano, Aline. C. Planello, Sergio R.P. Line, Ana Paula de Souza

Department of Morphology, School of Dentistry of Piracicaba, University of Campinas – UNICAMP, Av. Limeira, 901, 13414-018 Piracicaba, SP, Brazil

ARTICLE INFO

Article history:
Received 9 February 2015
Received in revised form
14 May 2015
Accepted 19 May 2015
Available online 30 May 2015

Keywords:
Anchorage blockade
Epigenetics
DNA methylation
Reactive oxygen species
Oxidative stress
Anoikis-resistance

ABSTRACT

Cell adhesion plays an important role in neoplastic transformation. Thus, anchorage-independent growth and epithelial-mesenchymal transition, which are features associated to anoikis-resistance, are vital steps in cancer progression and metastatic colonization. Cell attachment loss may induce intracellular oxidative stress, which triggers DNA damage as methylation changes. HaCaT lineage cells were submitted to periods of 1, 3, 5 and 24 h of anchorage blockage with the purpose of study of oxidative stress effect on changes in the DNA methylation pattern, derived from attachment blockade. Through this study, HaCaT anchorage blockage-induced oxidative stress was reported to mediate alterations in global DNA methylation changes and into *TP53* gene promoter pattern during anoikis-resistance acquisition. Furthermore, at the first experimental time-periods (1, 3 and 5 h), genome hypermethylation was found; however, genome hypomethylation was observed in later time-periods (24 h) of attachment impediment. The *TP 53* methylation analyses were performed after 24 h of replated anoikis-resistance cells and same methylation pattern was observed, occurring an early (1 and 3 h) hypermethylation that was followed by late (5 and 24 h) hypomethylation. However, LINE-1, a marker of genomic instability, was perceived in time-dependent hypomethylation. The mRNA levels of the DNMTs enzymes were influenced by cell attachment blockage, but non-conclusive results were obtained in order to match DNMTs transcription to pattern methylation results. In conclusion, DNA damage was found, leaded by oxidative stress that has come up from HaCaT anchorage blockade, which rises a global genome hypomethylation tendency as consequence, which might denote genomic instability.

1. Introduction

Epithelial cells depend on appropriate cell-matrix attachment to survive and to maintain their ordinary homeostasis, controlling appropriate tissue turnover. When the epithelial anchorage to extracellular matrix is lost, epithelial and endothelial cells experiment the apoptosis phenomenon termed anoikis [1]. This phenomenon is a programmed cell death, induced upon cell detachment from extracellular matrix, behaving as a critical mechanism in preventing adherent-independent cell growth and attachment to an inappropriate matrix, thus avoiding colonizing of distant organs [2]. Anchorage-independent growth and epithelial-mesenchymal transition, features associated with anoikis-resistance, are vital steps to cancer progression and metastatic colonization [3]. Thus, these features are some of tumor cells hallmarks which lead to the increase of cells lifetime and corroborates with epithelial-mesenchymal transition events; in a second step, metastatic malignant cells can reattach in (an)other site(s) [1].

Metastasis of cancer cells to distant sites in the body is responsible for the vast majority of cancer-related passings. Several studies have revealed that the loss of attachment to ECM gives up distinct variety of cellular and molecular alterations which ultimately contribute to the viability of ECM detached cells [4]. Hence, blockade epithelial attachment *in vitro* (anchorage blockade) has been employed as an alternative model to detachment resistance studies [5,6]. The adverse conditions of anchorage blockade result in oxidative stress, which leads to serious damage to cell constituents, including DNA, proteins and lipids. It is well known that DNA is targeted by reactive oxygen species (ROS) which originate multiple oxidative products able to mutate purine, pyrimidine and deoxyribose, such as the well-known oxidative damage DNA marker 8-hydroxy-2′-deoxyguanosine (8-OHdG) [7].

Reports have suggested that oxidative stress affects the epigenetic machinery, promoting chemical modifications into chromatin, including DNA methylation changes. DNA methylation represents the

* Corresponding author.
E-mail address: dasilva.rodrigo.a@gmail.com (R.A. da Silva).

http://dx.doi.org/10.1016/j.bbrep.2015.05.008

addition of methyl radicals (CH_3) to cytosine residues in the context of CpG dinucleotides, especially in CpG-rich regions termed as CpG islands [8]. This process is achieved by working of a group of enzymes named DNA methyltransferases (DNMT1, 3A and 3B) that have the nucleosome as substrate [9]. CpG islands are enriched in regulatory regions such as promoters and near the transcription start site (TSS). It is well known that DNA methylation represents an important mechanism within carcinogenesis since methylation may completely silence tumor suppressor genes [8]. Recently, an *in vitro* anoikis-resistance model was developed to induce murine melanocytes transformation [6]. After submitting non-tumorigenic melan-a cells to a battery of anchorage blockade cycles (5 sequential anchorage blockades of non-tumorigenic melan-a melanocytes), transformed melanoma cell lineage was obtained (4C11− and 4C11+), which became tumorigenic and contained dramatically methylated-altered genome [5].

Based on this previous study, the hypothesis of human keratinocyte cell line HaCaT anchorage-blockage was tested, to also lead to oxidative stress and DNA methylation changes. Our results report anchorage blockage consequences on oxidative stress, DNA damage, global DNA methylation pattern, LINE-1 sequence and *TP53* gene, as well as the impact over DNMTs transcription.

2. Materials and methods

2.1. Materials

Dulbecco's Modified Eagle's medium (DMEM), penicillin, streptomycin and fetal calf serum (SFB) were purchased from LGC Biotecnologia Ltda (São Paulo, SP, Bz). Tween, bovine serum albumin (BSA), [3-(4,5-dimethylthiazol-2-yl)-2,5-diphenyltetrazolium bromide] (MTT), specific primers, sodium dodecyl sulfate (SDS), Trizma, Tween 20, acrylamide, Bis-acrylamide, primers and catalase were acquired from Sigma Chemical Co. (St. Louis, MO, USA). OxyDNA Kit was obtained from Calbiochem (Mill Valley, CA, USA). Primary antibodies anti-5-Methyl Cytosine (*5*-meC) was obtained from CALBIOCHEM (©Merck KGaA) (Darmstadt, Hesse, DE). Secondary antibodies anti-mouse IgG conjugated with PE and anti-rabbit IgG conjugated with FITC were obtained from BD Bioscience (San Jose, CA, USA). Proteinase K, *Platinum® Taq DNA Polymerase,* phenol, chloroform, Alexa Fluor 633-conjugated wheat germ agglutinin (WGA633), dichlorodihydrofluorescein diacetate (H_2-DCFDA) and boron-dipyrromethene (C11-BODIPY581/591) were acquired from Invitrogen/Molecular Probes, Inc. (Eugene, OR, USA). Bisulfite Conversion Kit (MethylSEQr™) was purchased from Applied Biosystems (Van Allen Way, Carlsbad, CA). E*ndonucleases TaqI and TasI* were purchased from MBI-Fermentas (Burlington, Ontario, CA). GelRed™ was obtained from Biotium Inc. (Hayward, CA, EUA).

2.2. Methods

2.2.1. Cell culture and anchorage blockade

The human keratinocyte cell line HaCaT was provided by Dr. Carmen Veríssima Ferreira (Biology Institute, University of Campinas, São Paulo, Brazil). The cells were cultured in Dulbecco's Modified Eagle's medium (DMEM; Sigma Chemical Co.) supplemented with 10% fetal calf serum, 100 U/mL of penicillin and 100 μg/mL of streptomycin at 37 °C in a humidified atmosphere containing 5% CO_2. Viability and cell density were determined by the trypan blue dye exclusion test and sub cultured during 3 days. For anchorage blockade assays, adherent HaCaT cells were removed from plates via trypsin treatment (D0) and re-plated (10^5 cells/mL) on 1% agarose-coated dishes for 1, 3, 5 and 24 h (D1, D3, D5 and D24). Anchorage blockade effects on cell viability were evaluated by MTT reduction assay (MTT) as previously described [10]. Results were expressed as percent of cell viability of untreated control cells (D0) (100%).

2.2.2. Catalase cytotoxicity assay

HaCaT cells (3.5×10^4/well) were seeded in sextuplicate into 96-well plates in DMEM supplemented with 10% FCS and antibiotics. After 24 h of incubation at 37 °C in a humidified atmosphere containing 5% CO_2, the medium was replaced and cells were then treated with different catalase concentrations (0.05–2 mg/mL) in DMEM supplemented with 10% FCS, while control samples were treated with the corresponding volume of catalase-free culture medium. All samples were incubated for 24 h at 37 °C in a humidified atmosphere containing CO_2 at 5%. After treatment, cell viability was evaluated through MTT reduction assay (MTT). The results were expressed as percent of cell viability of untreated control cells (100%).

2.2.3. Assessment of redox status

2.2.3.1. Analysis of intracellular ROS presence and lipoperoxidation by flow cytometry and confocal microscopy. Intracellular ROS presence and lipoperoxidation were investigated by means of flow cytometry and confocal microscopy after incubation with specific probes. One hour previous to the end of treatment, 1 μM DCFDA and C11-BODIPY581/591 were added to cell cultures. Cells were then washed with PBS and fixed in paraformaldehyde 2% in PBS for one hour. For flow cytometry analysis, cells were washed in PBS, re-suspended in 300 μl PBS and analyzed (10.000 events were collected per sample) using FACSCalibur flow cytometer (Becton Dickinson, CA, USA) through CellQuest software (BD). Cells membranes were labeled with 10 μg/ml Alexa Fluor 633-conjugated WGA (WGA633) for 30 min, in order to confirm evidence of ROS presence and lipid peroxidation with confocal microscopy analysis. Cells were placed onto Cell-Tak coated glass coverslips, washed in PBS and mounted in Fluoromount-G. Cells were then analyzed using inverted laser scanning confocal microscope (Zeiss LSM 510 Confocal Microscope, Jena, Germany). The H_2-DCFDA was excited with a 488 nm argon laser and emission was detected by means of a bypass filter at 500–550 nm, and WGA633 was excited with a HeNe laser (excitation=633 nm) and light emission was detected at 635–700 nm. For lipoperoxidation analysis, BODIPY C11 was excited with 488 nm laser and emission was detected via bypass at 495 to 540 for the oxidized form and 550–610 for the non-oxidized form the BODIPY molecule. Examiner 4.2 (Zeiss) and Adobe Photoshop 9.2 were the software used for image preparation

2.2.3.2. Measurement of 8-OHdG by flow cytometry. The levels of 8-OHdG, a DNA damage marker for oxidative stress, were measured by means of specific OxyDNA Test kit conjugated to fluorescein isothiocyanate (FITC). After anchorage blockade, the cells were washed in PBS and fixed in paraformaldehyde 2% in PBS for 1 h. After permeabilization in PBS containing 0.2% Triton-X 100 and 1% BSA for one hour at room temperature, the cells were washed with Wash Solution and marked according to instructions (Calbiochem). The intensity of FITC fluorescence was measured with flow cytometer (10.000 events were collected per sample) using FACSCalibur flow cytometer (Becton Dickinson, CA, USA) through CellQuest software (BD).

2.2.4. Levels of Long Interspersed Nuclear Element-1 (LINE-1) methylation via COBRA PCR analysis

The genomic DNA was purified using the phenol/chloroform/isoamilic alcohol sequence protocol. The purified gDNA was modified by sodium bisulfite treatment using MethylSEQr™ Bisulfite Conversion commercial kit, according to manufacturer's instructions (Applied Biosystems). The modified DNA was eluted in 50 μL of 1.0 mM TE buffer (pH 7.6). The bisulfite-treated DNA was

submitted to 40 cycles of PCR using the follow primers set: foward 5′-CCGTAAGGGGTTAGGGAGTTTTT-3′ and reverse 5′-RTAAAACCCTCCRAACCAAATATAAA-3′ at the annealing temperature of 50 °C, aiming to generate 160 bp amplicons. Amplicons were further digested with *Taq*I (2 U) and *Tas*I (2 U) in *Taq*I buffer (MBI Fermentas) at 65 °C overnight. The methylated amplicons, *Taq*I positive, yielded two 80 bp DNA fragments; whereas the unmethylated amplicons, *Tas*I positive, yielded 63 and 97 bp fragments. After digestion, samples were electrophoresed in an 8% non-denaturing polyacrylamide gel, stained with GelRed (Biotium) and the intensities of the LINE-1 fragments in the polyacrylamide gel were quantified through a photo-imager (MultiDoc-It™ Imaging System) and graphics software/Scion Image (Scion Corporation). The details for band intensity quantitation were fully described elsewhere [11].

2.2.5. Analysis of 5-methylcytosine (5-meC) content by flow cytometry

After anchorage blockade, HaCaT cells were harvested by centrifugation, washed with PBS and fixed in paraformaldehyde 2% in PBS for 1 h at room temperature. Cells were then permeabilized in PBS containing 0.2% Triton-X 100 and 1% BSA for 1 h at room temperature and washed with PBS. For 5-meC evaluation, cells were incubated for 1 h at room temperature with 50 µl of specific primary antibody to 5-meC (Calbiochem) at final concentration of 1 mg/ml, followed by incubation for one hour in the dark and at room temperature with anti-mouse IgG PE-conjugated and anti-rabbit IgG FITC-conjugated secondary antibodies (BD Bioscience). The antibodies were diluted according to manufacturer's instructions. Cells were then washed in PBS, resuspended in 300 µl PBS and analyzed (10.000 events were collected per sample) using FACSCalibur flow cytometer (Becton Dickinson, CA, USA) through CellQuest software (BD).

2.2.6. RNA isolation and real-time quantitative-polymerase chain reaction (RT-PCR)

Total RNA was extracted from adherent (D0) and deadherent (D1, D3, D5 and D24) HaCaT cells with TRIzol reagent (Invitrogen, Carlsbad, CA). Previously, 2 µg of total RNA was treated with DNase (Invitrogen, Carlsband, CA, USA) and followed by input for cDNA synthesis with Superscript II (Invitrogen) according to manufacturer's instructions. The reaction of qPCR carried out in a total volume 10 µl, containing SYBR Green I Master 1 × (5 µl) (LightCycler® 480, Roche Applied Science, 250 nM of each primer, 2 µL of cDNA and nuclease free H_2O. PCR conditions were: 95 °C for 10 min, 45 cycles at 95 °C for 10 s. Primers and annealing temperature to amplify reference gene (GAPDH) along DNMT1, DNMT3A, and DNMT3B are described in Table 1. The qPCRs were performed at Light Cycler 480 II (Roche). Determination of relative levels of gene expression was performed using the cycle threshold (Ct) method in reference to GAPDH gene expression.

2.2.7. TP53 methylation analysis by methylation-sensitive restriction enzymes

To evaluate the *TP53* methylation status of anoikis-resistance cells, HaCaT cells were exposed to anchorage blockade for 1, 3, 5 and 24 h as described above and after different time-points, cells were re-plated in normal conditions. After 24 h in culture, the cells were washed with PBS and trypsinized and the gDNA was extracted using the phenol/chloroform/isoamilic alcohol sequence protocol. For *TP53* gene analysis, gDNA was initially digested by *HpaII* enzyme at 37 °C for 16 h, which recognized the restriction site (CCGG). *HpaII* enzyme is sensitive to methylation and CpG methylation blocks enzyme activity. After *HpaII* treatment, the templates were subjected to semi-quantitative PCR in order to compare methylation levels in the different groups. Therefore, a specific number of cycles of PCR reaction were defined at the exponential phase of amplification. An aliquot of 50 ng (10 µl) of the digested product was then used as template in PCR reaction: 12.5 µl Green Master Mix, 1 µl each primer: 5′-CTCCCCAACTCCATTTCCTT-3′ and antisense 5′-TGGACGGTGGCTCTAGACTT-3′, with 186 bp. The PCR was performed for 28 cycles under the following conditions: 95 °C, 5 min, 30 × (95 °C, 1 min; 62 °C, 1 min; 72 °C, 1 min), 72 °C, 7 min. Then, a 5 µl PCR reaction was electrophoresed on polyacrylamide gel, stained with SYBR Gold and photographed. Amplified DNAs of *TP53* gene were used as controls for restriction enzymes. An input of 100 ng of amplified DNA was submitted to restriction of each enzyme in order to ensure their effectiveness. The non-enzyme treated control DNA sample was always amplified with the primers, in parallel with the enzyme-treated samples, and both were subjected to electrophoresis in adjacent lanes. This provided a positive control for the PCR reaction and for DNA loading.

The intensity of the bands related to the samples are be obtained using Scion Image software and results are shown in percent as mean ± standard deviation. Our relative quantification considered that non-digested samples represented the totally amplified DNA template (100% of the initial template copies were amplified). Ttis way, the value of the quantification of enzyme-digested samples was subtracted from the value of the quantification of non-digested samples. This difference is the relative value of the not amplified unmethylated DNA. Therefore, methylation levels were classified into three groups: unmethylated = when the intensity of band matched from 0% to 25% of undigested DNA PCR band (0–25% of methylation); partially methylated = when the intensity of band matched from 25% to 75% of undigested DNA PCR band (25–75% of methylation); Methylated = when the intensity of band matched from 75% to 100% of undigested DNA PCR band (75–100% of methylation). DNA samples which were not treated with restriction enzyme were considered as control template, representing 100% of input DNA amplified after PCR.

Table 1
Expression primers sequences and PCR cycle conditions l.

Gene	Primer	Sequence	Annealing temperature	Extension temperature	Fragment
GAPDH	**Forward**	**5′-CCA CTCCTCCAC CTTTGA C-3′**	**56 °C**	**15 s**	**103 bp**
	Reverse	**5′-ACC CTGTTGCTG TAGCCA-3**			
DNMT1	**Forward**	**5′-ACC TGGCTAAAG TCAAAT CC-3′**	**56 °C**	**20 s**	**80 bp**
	Reverse	**5′-ATT CACTTCCCG GTTGTA AC-3′**			
DNMT3A	**Forward**	**5′-GAA GGACTTGGG CATTCA GGT-3′**	**56 °C**	**20 s**	**105 bp**
	Reverse	**5'-CCGACGTAC ATGATCTTC CC-3'**			
DNMT3B	**Forward**	**5′-CGA GTCCTGTCA TTGTTTGAT GG-3′**	**56 °C**	**20 s**	**60 bp**
	Reverse	**5′-GCG ACGTACTTT CCTACCTTT ATG-3′**			

In all runs, a negative control containing master mix, RNA free water and primers, but no cDNA, was included. All reactions were made in duplicate, both genes of interest – *DNMT1, DNMT3A* and *DNMT3B* – as for the housekeeping gene – *GAPDH*. The analysis of melting curves were performed on heating ramp from 65 °C to 95 °C with 25 acquisitions/°C. **F**= forward; **R**= reverse.

3. Statistical analysis

All tests were performed in three independent experiments and analyzed in duplicate. Results were expressed as mean ± standard deviation. Statistical analysis was performed by the Student's *t*-test, or analysis of variance (ANOVA) followed by the post hoc Tukey test when more than two groups were compared using Instat software (SigmaStat for Windows version 3.1, Systat Software Inc., USA). Differences were considered significant at $P < 0.05$, representing two-sided test of statistical significance. Densitometric analysis of bands was performed using the Scion Image software.

4. Results

4.1. Anchorage blockade induced reactive species of oxygen (ROS) generation in keratinocytes

The non-tumorigenic human keratinocyte lineage HaCaT was submitted to anchorage blockade through blocking adhesion to substrate, as described above. After 1, 3, 5 and 24 h of anchorage blockade, the cell viability was evaluated by MTT reduction in adherent (D0) and deadherent HaCaT cells (D1, D3, D5 and D24). As shown in Fig. 1A, HaCaT cells reached 50% of viability (IC_{50} value) only after 24 h of anchorage blockade. Following, the emergence of oxidative stress induced by blocking adhesion on keratinocytes was investigated. The analysis of intracellular ROS production was performed by flow cytometry and confocal microscopy, using the oxidation-sensitive fluorescent probe DCFH-DA. The diacetate form of DCF (H_2-DCFDA) is taken up by cells and hydrolyzed to membrane-impermeant dichlorofluorescein (DCFH), which is oxidized in the presence of ROS to form the highly fluorescent dichlorofluorescein (DCF). As shown in Fig. 1B (Anchorage Blockade) and Fig. 1C, significant increase in the intracellular ROS production was observed in a time-dependent manner after blocking adhesion when compared to control cells (adherent – D0). Considering that ROS may be involved in the cytotoxic effects observed by anchorage blockade, the HaCaT cells were pre-treated with catalase. In order to test if catalase pre-treatment was able to avoid the cytotoxic effects of anchorage blockade, the catalase cytotoxicity after a 24-h incubation period using the colorimetric MTT assay was initially evaluated. The results (data not shown) showed that catalase was not cytotoxic at concentrations below 2.0 mg/ml. Then, to confirm the catalase cytoprotective potential, HaCaT cells were submitted to anchorage

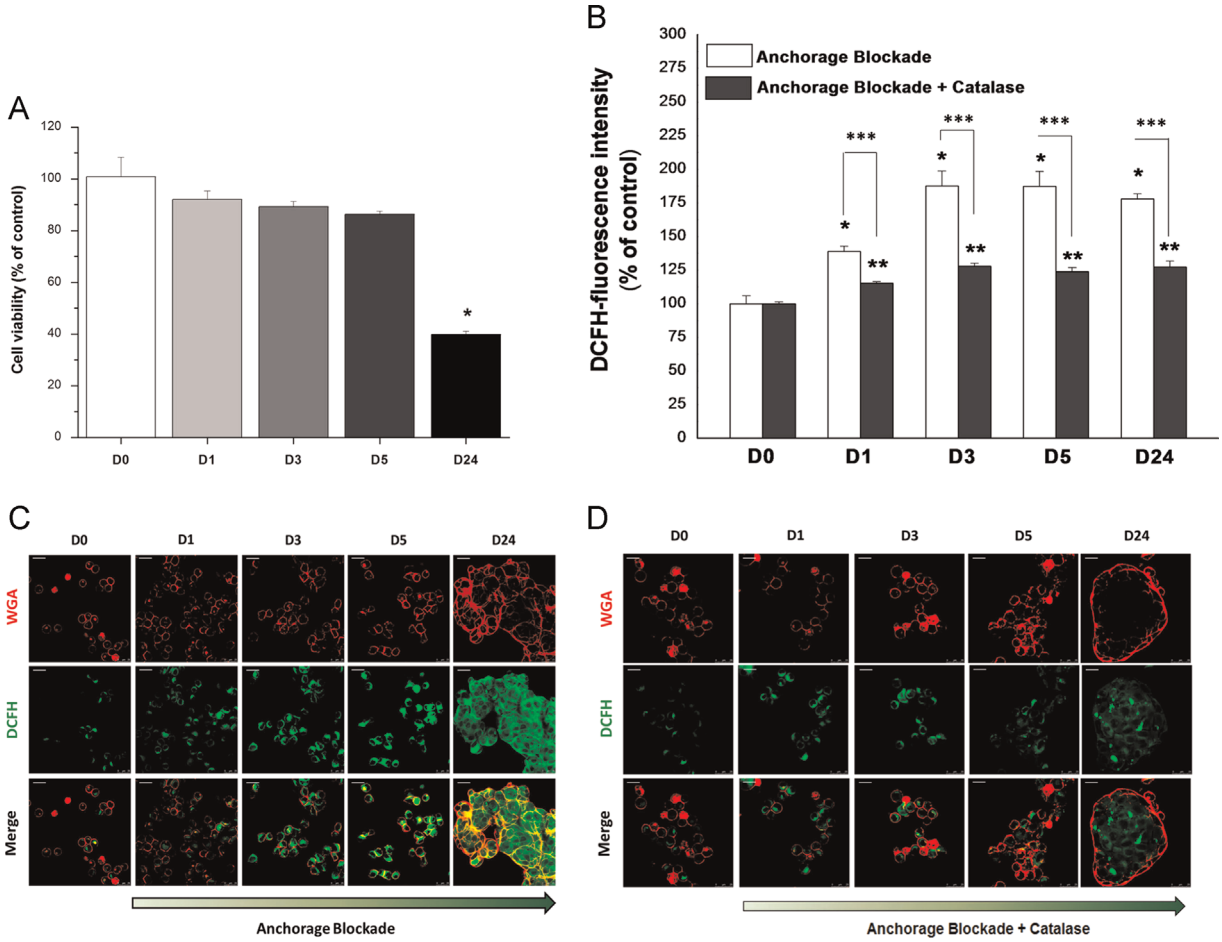

Fig. 1. Effects of anchorage blockade on cell viability and intracellular ROS production. (A) HaCaT plated on blocking adhesion to substrate for 1, 3, 5 and 24 h (D1, D3, D5 and D24). After anchorage blockade the cells were re-plated in normal growth conditions, and cellular viability was assessed after 24 h by MTT reduction. The results were expressed as percentage of control (D0) cell viability (100%) and represented as mean ± SD of three independent experiments run in triplicate. (B) Significant increase of intracellular ROS production was detected by flow cytometry in suspended (D1, D3, D5, and D24) when compared to control cells (D0) using the oxidation-sensitive fluorescent probe DCFH-DA during anchorage blockade. (C) Confocal microscopy of intracellular ROS using the oxidation-sensitive fluorescent probe DCFH-DA. Anchorage blockade significantly increases intracellular ROS production in a time-dependent manner compared with control cells (D0 and D) catalase treatment affected ROS production during anchorage blockade. Membranes were stained with WGA633. Images are representative of three independent experiments. Bars = 20 μm.*$P < 0.05$ compared with control D0 (Anchorage Blockade), **$P < 0.05$ compared with control D0 (Anchorage Blockade + Catalase) and ***$P < 0.05$ compared between anchorage blockade and Anchorage Blockade + Catalase groups.

blockade in medium containing 0.2 mg/ml of catalase. The results from flow cytometry assay and confocal microscopy assay showed that catalase significantly reduced ROS generation during different periods of cell adhesion blockade when compared to control cells (adherent – D0) ($P < 0.05$) (Fig. 1B – Anchorage Blockade + Catalase and Fig. 1D, respectively).

4.2. Oxidative stress promotes lipid peroxidation, oxidative DNA-lesions and genomic instability during anchorage blockade

ROS can damage not only DNA, but also other cellular components such as lipids. In consequence, the application of lipid peroxidation using fluorescent probe method C11-BODIPY581/591 was investigated, as previously described by Pensalfini and collaborators [12]. Lipid peroxidation after anchorage blockade was also investigated by flow cytometry and confocal scanning microscopy. In particular, C11-BODIPY581/591 by mimicking the properties of natural lipids [13] can be used to measure antioxidant activity in lipid environments, since it behaves as a fluorescent lipid-peroxidation reporter that shifts its fluorescence from red to green when challenged with oxidizing agents [14]. After the cells anchorage blockade assay, a gradual reduction of the red fluorescence (Fig. 2A – Anchorage Blockade) followed the concomitant green fluorescence increase (Fig. 2B – Anchorage Blockade) were observed through flow cytometry analysis, which provided indication of lipid peroxidation. Using confocal microscopy, the oxidation of C11-BODIPY581/591 can have been at cellular level. Over time, in the presence of normal cellular membranes, the C11-BODIPY581/591 fluorophore maintained its red fluorescence (610 nm) and presented no green fluorescence (510 nm). During anchorage blockade, the BODIPY fluorophore decreased in red fluorescence and increased in green fluorescence, confirming membrane oxidation (Fig. 2C). After confirmation of lipid peroxidation, the ROS-mediated DNA damage was investigated by dint of measuring the genome 8-OHdG levels. Aiming to explore the presence of oxidized bases which could be

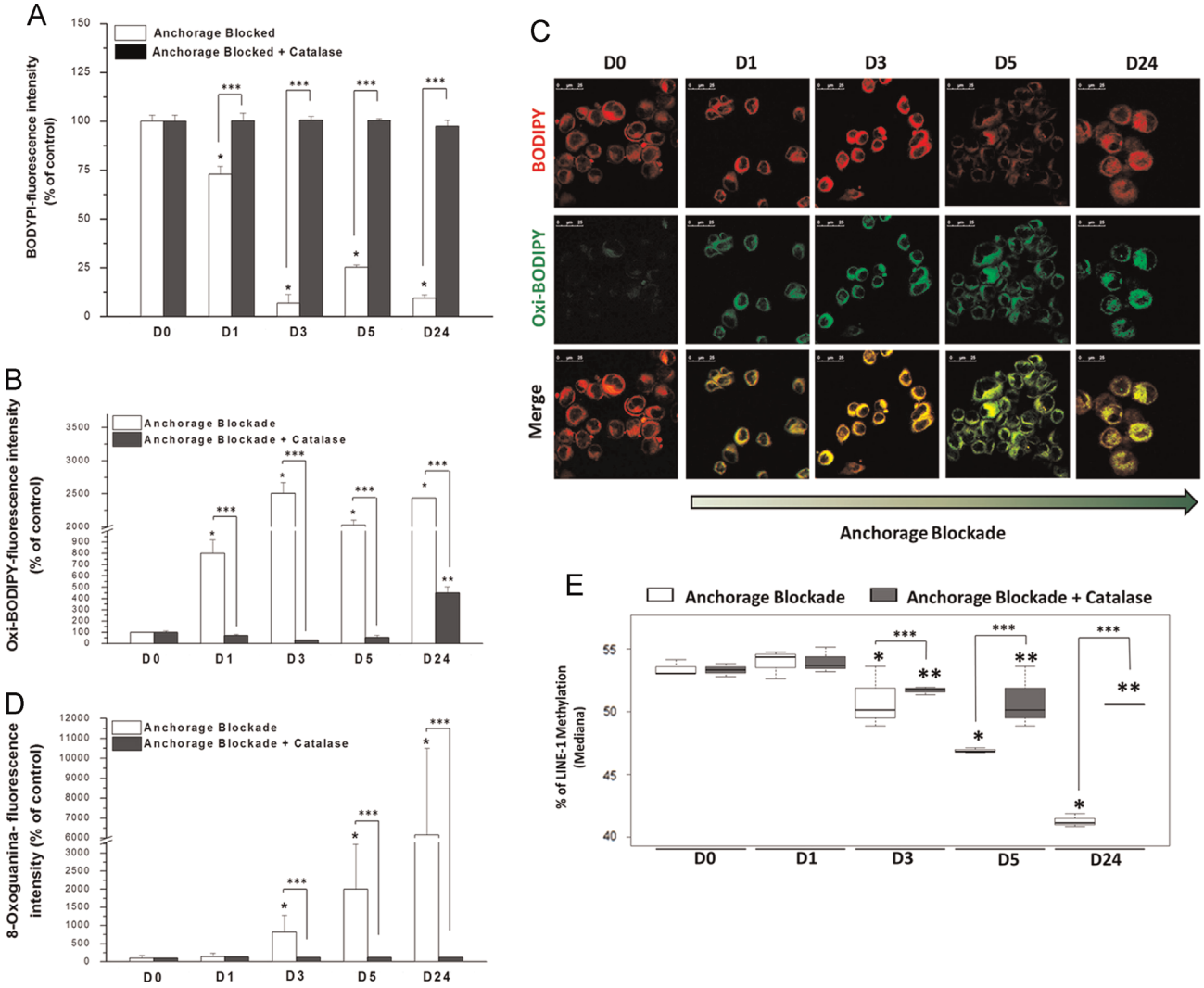

Fig. 2. Anchorage blockade-induced HaCaT cell damage oxidative is mediated by oxidative stress. Lipid peroxidation was analyzed by flow cytometry and confocal microscopy in suspended (D1, D3, D5, and D24) and adherent (D0) HaCaT using the oxidation-sensitive fluorescent probe C11-BODIPY581/591. The oxidation of C11-BODIPY581/591 fluorophore is monitored simultaneously at 510 nm and 610 nm, A and B respectively. (A) Flow cytometry analysis demonstrated significant reduction in the intensity of red fluorescence (nonoxidized probe), and (B) increased fluorescence intensity of green fluorescence (oxidized probe). (C) Fluorescence micrographs obtained by confocal microscopy analysis revealed increased lipid peroxidation in a time-dependent manner compared with control cells (D0). Images are representative of three independent experiments. Bars = 20 μm. (D) Flow cytometry analysis showing oxidative DNA damage. Note a time-dependent increase in fluorescence intensity of the 8-OHdG during anchorage blockade. (E) Comparison of the percentages of methylation patterns of LINE-1 detected by COBRA PCR in HaCaT cells during anchorage blockade and Anchorage Blockade + Catalase. Black horizontal bars represent the median (IQR). The results were expressed as percentage of control (D0) lipid peroxidation and oxidative DNA-lesions (100%) and represent the mean ± SD of three independent experiments run in triplicate.*$P < 0.05$ compared with control D0 (Anchorage Blockade), **$P < 0.05$ compared with control D0 (Anchorage Blockade + Catalase) and ***$P < 0.05$ compared between Anchorage Blockade and Anchorage Blockade + Catalase groups.

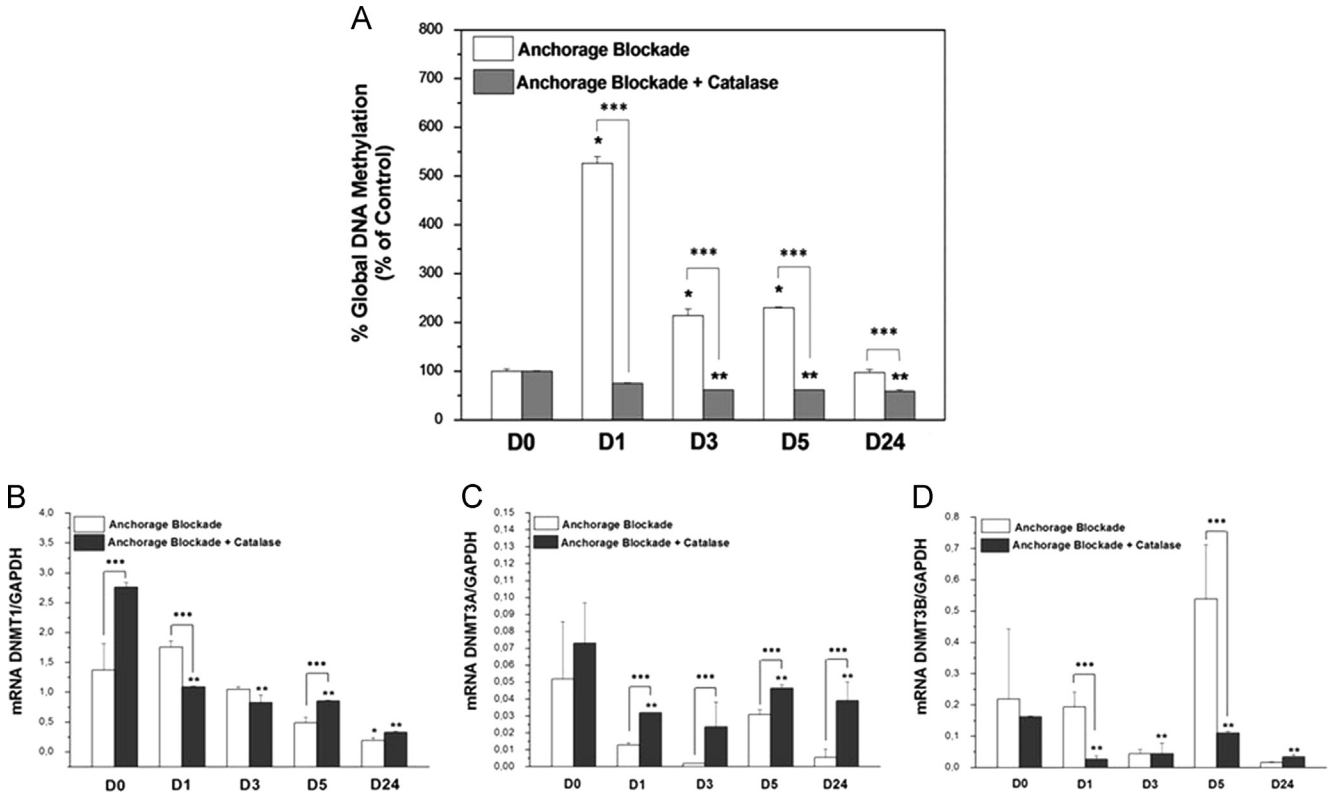

Fig. 3. Global DNA methylation and DNMTs expression levels during Anchorage Blockade. Total global DNA methylation and DNMTs expression levels were evaluated by flow cytometry and RT-PCR analysis in HaCaT cells exposed to blockade adhesion to substrate for 1 to 24 h, compared to the adherent cells (D0). (A) The effects of Anchorage Blockade on global DNA methylation were also demonstrated by flow cytometry analysis of cells stained with anti-5-meC specific antibody (Calbiochem). Results were represented as mean ± standard deviation of three independent experiments. (B–D) The levels of DNMT1 (A), DNMT3A (B) and DNMT3B (C) mRNA detected by RT-PCR analysis. Expression was normalized to GAPDH mRNA levels. Results were represented as mean ± standard deviation of three independent experiments performed in duplicate. $^{*}P<0.05$ compared with control D0 (Anchorage Blockade), $^{**}P<0.05$ compared with control D0 (Anchorage Blockade+Catalase) and $^{***}P<0.05$ compared between Anchorage Blockade and Anchorage Blockade+Catalase groups.

produced by oxidative events during anchorage blockade, the 8-OHdG levels were determined by flow cytometry. As disclosed in Fig. 2D, anchorage blockade promoted genotoxicity, as demonstrated by the increased fluorescence intensity of 8-OHdG.

Therefore, Combined Bisulfite Restriction Analysis (COBRA) assay was performed to assess the methylation levels of LINE-1 in different periods of blocking cell adhesion. Statistical differences were found and results clearly revealed hypomethylation tendency in a time-dependent manner in response to anchorage blockade (Fig. 2D). In an additional set of studies, catalase was added to the cells during anchorage blockade as a test to determine if the oxidative damage to HaCaT cells could be prevented. Results demonstrated that lipid peroxidation did not occur when HaCaT cells were submitted to anchorage blockade in the presence of catalase (Fig. 2A and B – Anchorage Blockade+Catalase); thus, preventing the occurrence of oxidative DNA-lesions and LINE-1 hypomethylation events during to anchorage blockade (Figs. 2D and 3E – Anchorage Blockade+Catalase).

4.3. Catalase treatment prevents DNA methylation changes during anchorage blockade

Blocking adhesion to substrate promoted increase in global DNA methylation levels (5-fold) in suspended HaCaT cells (D1) when compared to adherent ones (D0) (Fig. 3A – Anchorage Blockade). However, after the first hour, the 5-meC levels progressively decreased, maintaining the hypermethylation status during 3 and 5 h while in suspension (D3 and D5) and normalizing up to 24 h (Fig. 3A – Anchorage Blockade). Since the increase in ROS production and hypermethylation events have direct association in this model, the effect of catalase treatment during the anchorage blockade in global DNA methylation levels was evaluated. Results showed that catalase completely prevents 5-meC increase levels during all periods (D1, D3, D5 and D24) of cells suspension if compared to control cells (D0) confirming the involvement of oxidative stress in this process (Fig. 2A – Anchorage Blockade+Catalase).

4.4. DNA methyltransferases (DNMTs) expression during HaCaT anchorage blockade

In order to determine if the altered level of DNA methylation observed during blocked anchorage is associated to differential expression of DNMTs, DNMT1, 3A and 3B mRNA content at different time-points (D0, D1, D3, D5 and D24)were evaluated. Results showed mild increase of DNMT1 mRNA in D1 when compared to D0 (catalase free-medium) and reduction when compared to other time-points (Fig. 3B). In turn, DNMT3B mRNA reached significant increase in D5 when compared to other time-points (catalase free-medium) ($P<0.05$) (Fig. 3D). No differences were found in DNMT3A (Fig. 3C). Results showed that catalase treatment promotes significant decrease in DNMTs mRNA levels during anchorage blockade (Fig. 3B–D) (Anchorage Blockade+Catalase).

4.5. TP53 methylation pattern

The methylation status of a CpG site-specific into *TP53* gene promoter in anoikis-resistance cells was investigated in order to verify the methylation status of a specific gene which takes part in

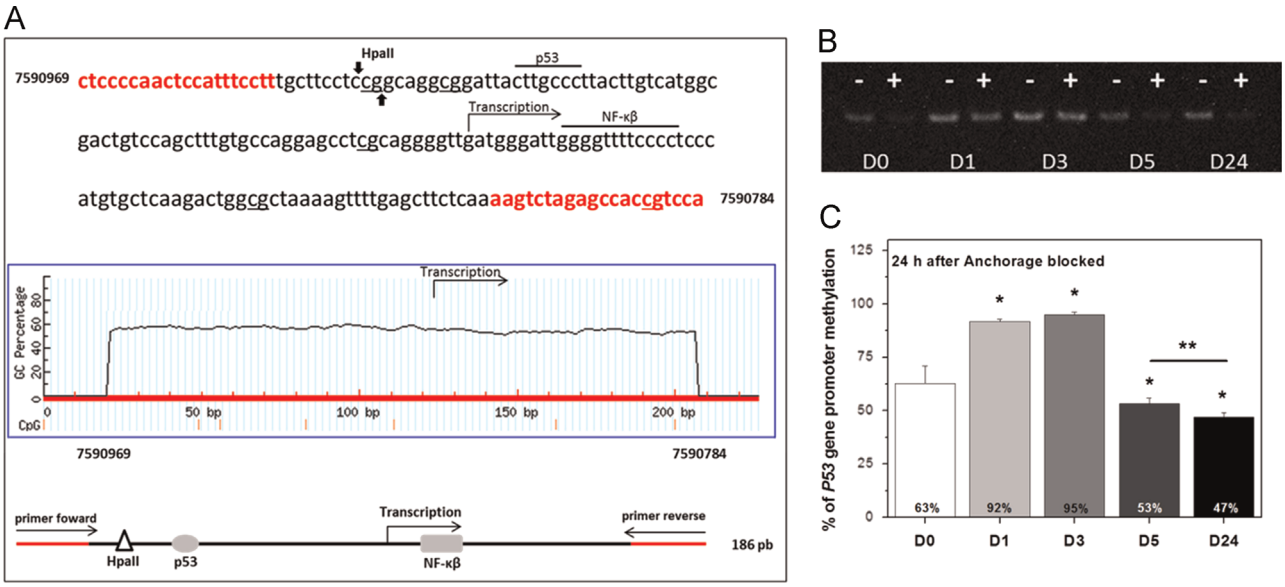

Fig. 4. *P53*gene promoter methylation analysis in anoikis-resistant HaCaT cells. After different time-points of anchorage blockade (D1, D3, D5 e D24) the cells were re-plated and anoikis-resistant HaCaT cells were cultured in adherent normal conditions. After 24 h of the re-plated the *P53* methylation pattern in anoikis-resistant cells were performed by specific restriction endonuclease digestion as described in Section 2. (A) Schematic representation of amplified region of *P53* gene. The sequence amplified shows primers set in red and underlined bases containing CG dinucleotide show sequences amenable to recognize by restriction enzymes *HpaII* (CCGG). (B) One representative electrophoresis of *HpaII*-PCR *P53* methylation. **(–)** indicates non-digested DNA samples and **(+)***HpaII*-digested DNA samples. (C) Densitometric analysis of the *P53* methylation after 24 h anchorage blocked. The percentage of *P53* gene promoter methylation is performed relation between band intensity to control samples (undigested) by intensity of *HpaII*-digested DNA samples. **T**he percentage of *P53* gene promoter methylation is performed by dividing the intensity of the band related to control samples (undigested) by band intensity on the HpaII enzyme digestion (methylation sensitive). Results were represented as mean ± standard deviation of three independent experiments performed in duplicate. $^{*}P < 0.01$ compared with control (D0) and $^{**}P < 0.05$ compared with control (D0) and anoikis-resistant cells (D1 and D3).

the cellular cycle control. The promoter region of *TP53* gene contains CpG sites placed between bases -277 and -91 (GenBank Accession Number J04238). *Hpa*II restriction site was placed upstream and represented the unique CCGG consensus sequence (Fig. 4A). Results showed *TP53* gene promoter was partially methylated (63%) in D0 group and then anchorage blockade promoted significant hypermethylation in groups D1 and D3 (92% and 95%, respectively) and hypomethylation in D5 and D24 if compared to *TP53* methylation pattern of HaCaT anoikis-resistance cell to control group (D0) (Fig. 4B).

5. Discussion

It is well known that cell–cell and cell–ECM interactions play crucial roles in controlling appropriate cellular functions. Thus, cell-detachment-induced apoptosis is a self-defense strategy used to eliminate 'misplaced' cells [1]. In this context, the anchorage blockade is an experimental model used in the anoikis resistance and carcinogenic transformation studies, by means of enabling the identification of biochemical, the genetic and epigenetic alterations involved in homeostatic loss control [6]. The efforts are primarily based in the belief that the use of experimental models which enables studies on how normal cells may respond to adherence lock will certainly help to decipher the role attributed to of the anoikis resistance and carcinogenic process.

In the present study, the effects promoted by de-attached model was analyzed by submitting the non-tumorigenic human keratinocyte lineage HaCaT cells to anchorage blockade for 1, 3, 5 and 24 h. The exposure of HaCaT cells to adhesion impediment induced oxidative stress from the moment increased levels of intracellular ROS production and lipid-peroxidation were found. Due to its characteristics, lipid components of the membranes are the preferential targets of oxidants species. The lipid peroxidation is able to trigger an autocatalytic cascade that generates numerous genotoxic substances, which are able to damage the integrity of the DNA [15]. Lipid peroxides, formed by the attack of radicals on polyunsaturated fatty acid residues of phospholipids, are able to react further with redox metals, finally producing mutagenic and carcinogenic malondialdehyde, 4-hydroxynonenal and other exocyclic DNA adducts [16].

In this context, 8-OHdG is one of the major forms of free radical-induced DNA oxidative lesions and it has, therefore, been widely used as a biomarker for oxidative stress. The results of this study clearly showed a time-dependent increment of 8-OHdG. After periods of 3, 5 and 24 h of anchorage blockade, the 8-OHdG levels in no-adherent cells (D0) have increased significantly if compared to their adherent counterparts (D3, D5, D24). In CpG dinucleotides, the cytosine is the preferred base for DNA methylation, whereas the guanine is the site for oxidative damage. Consequently, the oxidation of guanine to 8-OHdG converts the N7 position of guanine from a hydrogen bond acceptor into a hydrogen bond donor, as well as it replaces the 8-proton with an oxygen atom. Replacement of guanine to 8-OHdG diminishes MBP binding substantially when 8-OHdG is adjacent to the 5-methylcytosine and may promote genomic instability and DNA methylation changes [17].

LINE-1 hypomethylation in cancer cells is correlated to genome instability, leading to retro transposition activation, endogenous DNA double-strand break (EDSB) repair, and the dysregulation of DNA repair genes [18]. However, the relationship between increased oxidative stress and hypomethylation of LINE-1 is still completely unknown [19]. This study shows, for the first time, the relationship between LINE-1 hypomethylation and oxidative stress during the anchorage blockade and it has been found as one of the first evidences of anchorage blockade genomic instability promotion in normal human keratinocytes. LINE-1 is one amongst different types of transposable repetitive sequence elements and it represents approximately 17% of human genome; thus, LINE methylation investigation is widely considered and used to compose studies of global methylation. LINE hypomethylation is directly associated with increased genomic instability [11,18,20] and

reinforce the hypothesis of association between cellular redox state and changes in global DNA methylation pattern [16,21]. Oxidative stress and DNA methylation are metabolically linked by the relationship between the metabolism of one-carbon and the transsulfuration pathway Glutathione (GSH), a product of transsulfuration pathway donates one electron to reactive oxygen species;a reaction in which the enzyme glutathione peroxidase takes part [22]. However, in order to produce glutathione, the cell metabolism may promote disorders in the cycle of molecules which are implicated to produce S-adenosylmethionine (SAM), the main substrate of DNMTs, since GSH derived from Cys, a product of homocysteine (Hcy) that takes part within methionine cycle [21].

The current work emphasizes the importance of cellular redox state and changes in global DNA methylation. It is noteworthy that results demonstrated that oxidative stress is able to exert influence in genomic instability and DNA methylation patterns, promoting increase in the 5-methylcytosine levels in the trial. Another interesting phenomenon observed in this study which should be further explored is the progressive decrease in global 5-methylcytosine levels during 3 and 5 h and the equating of 5-methylcytosine levels after 24 h. Two working hypotheses can be generated; the existence of a "cellular epigenetic memory", which may be contributing to cellular epigenetic machinery and the restoration of the initial epigenetic patterns as a defense mechanism to maintain DNA methylation pattern. Studies show that increased oxidative stress causes DNA lesions resulting in increased DNA repair activity to reverse the global DNA methylation patterns changes [23,24]. However, we shall not affirm that epigenetic marks are the same as results herewith only showed global DNA methylation patterns after exposure to cell adhesion block for 24 h. Necessary Additional studies are required, with the view to assess the patterns and specific genes, aiming to confirm that cells exposed to blocked anchorage during a 24-h period do not evidence epigenetic changes, camouflaged by the normalization of global methylation patterns of observed DNA.

The maintained DNA methylation pattern in mammal cells is mainly by DNMT1 action of hemi-methylated parent–daughter duplexes during DNA replication and plays an important role in maintaining genomic stability and gene regulation [25–27]. For this reason, in this experimental model, the time period of 24 h was applied, mainly because the doubling time for this cell line is approximately 22 h. Curiously, data demonstrated that anchorage blockade-induced oxidative stress promotes global DNA hypermethylation during the adhesion impediment, but no correlate with the DNMTs gene expression in all the time-point was noticed. Importantly, the oxidation of guanine into 8-oxoguanine within a CpG dinucleotide or DNA damage may alter the specificity of DNMT1, either inhibiting the methylation of hemimethylated sites or triggering the inappropriate methylation of previously unmethylated sites [28].

Several aspects of dynamic action of DNMTs and TETs enzymes in the regulation of DNA methylation pattern have been described in different biological conditions. Of interest, the oxidative stress ability to modulate changes in the global DNA methylation during adhesion impediment in murine non-tumorogenic melanocyte by increase in DNMTs expression has been studied [6,29]. However, in human cells, this mechanism is undetermined and was not clear. Though, some studies suggest that DNMTs' overexpression could be responsible for hypermethylation observed in promoter regions of tumor suppressor in tumor cells during the carcinogenic process, but until now, this hypothesis is not clear [30,31]. Investigations demonstrated similar results were revealed inhibition of ROS production resulted in the decrease of DNMT upregulation and DNA methylation [32].

Campos and collaborators [6] had not observed differences between melan-a catalase treatment during adhesion impediment. Through this, it is believed that the difference in response may be due being different cell types with distinct biological functions. Differences were found after the HaCaT catalase-treatment in the DNMTs levels at all time-points in the experiments, including D0. It is probable that the difference after catalase-treatment in the D0 time-point is a result of existing oxidative stress background into the cells maintained in culture. In spite of the demonstration that oxidative stress modulated the levels of mRNA transcription of DNMTs and DNA methylation pattern [6], but in the experimental model it was not possible to have these variations directly correlated to the ones observed in global DNA methylation pattern, this fact may be related to experimental conditions. Acting together with the DNMTs in maintaining the DNA methylation pattern, there is the action of Ten-Eleven Translocation (TET)-family demethylases proteins (TETs) [24]. In this context, another possibility would be the oxidative stress upregulation TETs mRNA expression or activity promoting an imbalance in the action of DNMTs and TeTs, favoring observed hypermethylation.

In addition, detached or misplaced cells are able to overcome *anoikis* and survive for a certain period of time in the absence of the correct signals from the extracellular matrix (ECM). Nevertheless, if cells are able to adapt to their new environment, then they have probably become anchorage-independent, which is one of the hallmarks of cancer cells [33]. In this way, after confirmation of the changes shown above, effects of epigenetic alterations were investigated and observed during the adhesion impediment in the process of acquisition of anoikis resistance. Anoikis resistance and anchorage-independency allow tumor cells to expand and invade adjacent tissues to disseminate through the body, giving rise to metastasis. Thus, overcoming anoikis is a crucial step in a series of changes undergone by tumor cells during malignant transformation. Results demonstrated the anoikis-resistant HaCaT cells presented characteristics compatible to tumor cells, as *TP53* hypermethylation.

In order to know if HaCaT cell line has P53 mutation at dipyrimidine sites in codon 179 of exon 5 and 281 and 282 of exon 8 have been implicated in the mechanism of immortalization of this cell line [34]. However, one study demonstrated that blocking mutated p53 partially blocked UVB-induced apoptosis in HaCaT cell line and furthermore confirm the key role for p53 apoptosis in human keratinocytes. Moreover, these results clearly demonstrated that p53 must, at least in part, remain functional in spite of its mutation points in HaCaT [35]. Thus, our study demonstrates, for the first time in human cell line, results which indicate that the involvement of methylation in the *P53* gene promoter motivated by oxidative stress in experimental model of acquisition resistance anoikis.

Results support the possibility that the DNA methylation status changes were induced in cells selected for resistance to anoikis. It was shown that oxidative stress can have opposing effects on cell survival [36]. On the one hand, ROS production following cell detachment correlates with anoikis [37]. However, it is believed that this metabolic stress may be bypassed by the epigenetic inactivation of important tumor suppressor genes, as the *TP53* and activation of oncoproteins, which may be rescues the ATP deficiency by restoring glucose uptake [38]. In contrast, increased ROS production has been detected during metastasis, which is probably related to hypoxia and in this situation could have a protective effect, associated to the ability of ROS to elicit pro-survival signals [39]. The role of ROS in anoikis protection is likely to be dependent on several factors and also to be influenced by the potent crosstalk between integrins, growth factor signaling and DNA methylation. It is possible that in cells capable of survival without adhesion to the substrate, another set of genes is activated, thus a detailed study of DNA methylation dynamics during these processes is necessary and will greatly help to better tease apart the molecular events which occur during the anoikis-resistant HaCaT.

In summary, this work provides new contribution to the comprehension of mechanisms involved in the response of human keratinocytes during adhesion impediment and anoikis-resistant

acquisition. These results enrich the literature on the effects of ROS on global DNA methylation pattern; however, complementary studies are necessary to clarify how metabolic mechanisms influenced this process in normal keratinocytes upon exposure to anoikis-resistant model.

Competing interests

None declared.

Author contributions

Conceived and designed the experiments: RAS APS FSM ACP. Performed experiments: RAS FSM. Analyzed data: RAS APS ACP. Contributed with reagents/materials/analysis tools: RAS APS SRPL. Wrote the paper: RAS APS SRPL.

Acknowledgments

This study was supported by research grants from Fundação de Amparo à Pesquisa do Estado de São Paulo (FAPESP) (2010/08180-0). Da Silva RA was supported by FAPESP (2011/09498-6).

Appendix A. Supplementary Information

Supplementary data associated with this article can be found in the online version at http://dx.doi.org/10.1016/j.bbrep.2015.05.008.

References

[1] S.M. Frisch, M. Schaller, B. Cieply, Mechanisms that link the oncogenic epithelial-mesenchymal transition to suppression of anoikis, J. Cell Sci. 26 (2013) 21–29.
[2] P. Chiarugi, E. Giannoni, Anoikis: a necessary death program for anchorage-dependent cells, Biochem. Pharmacol. 76 (2008) 1352–1364.
[3] P. Paoli, E. Giannoni, P. Chiarugi, Anoikis molecular pathways and its role in cancer progression, Biochim. Biophys. Acta 2013 (1833) 3481–3498.
[4] C.L. Buchheit, K.J. Weigel, Z.T. Schafer, Cancer cell survival during detachment from the ECM: multiple barriers to tumour progression, Nat. Rev. Cancer 14 (2014) 632–641.
[5] F. Molognoni, A.T. Cruz, F.M. Meliso, A.S. Morais, C.F. Souza, P. Xander, J. M. Bischof, F.F. Costa, M.B. Soares, G. Liang, P.A. Jones, M.G. Jasiulionis, Epigenetic reprogramming as a key contributor to melanocyte malignant transformation, Epigenetics 6 (2011) 450–464.
[6] A.C. Campos, F. Molognoni, F.H. Melo, L.C. Galdieri, C.R. Carneiro, V. D'Almeida, M. Correa, M.G. Jasiulionis, Oxidative stress modulates DNA methylation during melanocyte anchorage blockade associated withmalignant transformation, Neoplasia 9 (2007) 1111–11217.
[7] B. Halliwell, Biochemistry of oxidative stress, Biochem. Soc. Trans. 35 (2007) 1147–1150.
[8] A.P. Bird, CpG-rich islands and the function of DNA methylation, Nature 321 (2013) 209–213.
[9] S. Sharma, D.D. De Carvalho, S. Jeong, P.A. Jones, G. Liang, Nucleosomes containing methylated DNA stabilize DNA methyltransferases 3A/3B and ensure faithful epigenetic inheritance, PLoS Genet. 7 (2011) e1001286.
[10] T. Mosmann, Rapid colorimetric assay for cellular growth and survival: application to proliferation and cytotoxicity assay, J. Immunol. Methods 65 (1983) 55–63.
[11] N. Kitkumthorn, T. Tuangsintanakul, P. Rattanatanyong, D. Tiwawech, A. Mutirangura, LINE-1 methylation in the peripheral blood mononuclear cells of cancer patients, Clin. Chim. Acta 413 (2012) 869–874.
[12] A. Pensalfini, C. Cecchi, M. Zampagni, M. Becatti, F. Favilli, P. Paoli, S. Catarzi, S. Bagnoli, B. Nacmias, S. Sorbi, G. Liguri, Protective effect of new S-acyl-glutathione derivatives against amyloid-induced oxidative stress, Free Rad. Biol. Med. 44 (2008) 1624–1636.
[13] Y.M. Naguib, A fluorometric method for measurement of peroxyl radical scavenging activities of lipophilic antioxidants, Anal. Biochem. 265 (1998) 290–298.
[14] G.P.C. Drummen, B.M. Gadella, J.A. Post, J.F. Brouwers, Mass spectrometric characterization of the oxidation of the fluorescent lipid peroxidation reporter molecule C11-BODIPY581/591, Free Rad. Biol. Med. 36 (2004) 1635–1644.
[15] B.A. Wagner, G.R. Buettner, C.P. Burns, Free radical-mediated lipid peroxidation in cells: oxidizability is a function of cell lipid bis-allylic hydrogen content, Biochemistry 33 (1994) 4449–4453.
[16] G. Barrera, S. Pizzimenti, M.U. Dianzani, Lipid peroxidation: control of cell proliferation, cell differentiation and cell death, Mol. Aspects Med. 29 (2008) 1–8.
[17] K.V. Donkena, C.Y. Young, D.J. Tindall, Oxidative stress and DNA methylation in prostate cancer, Obstet. Gynecol. Int. (2010) 302051.
[18] N. Kitkumthorn, A. Mutirangura, Long interspersed nuclear element-1 hypomethylation in cancer: biology and clinical applications, Clin. Epigenetics 2 (2011) 315–330.
[19] M. Patchsung, C. Boonla, P. Amnattrakul, T. Dissayabutra, A. Mutirangura, P. Tosukhowong, Long interspersed nuclear element-1 hypomethylation and oxidative stress: correlation and bladder cancer diagnostic potential, PLoS One 7 (2012) e37009.
[20] N.E. Lange, J. Sordillo, L. Tarantini, V. Bollati, D. Sparrow, P. Vokonas, A. Zanobetti, J. Schwartz, A. Baccarelli, A.A. Litonjua, D.L. Demeo, Alu and LINE-1 methylation and lung function in the normative ageing study, BMJ Open 17 (2012) e001231.
[21] M.M. Niedzwiecki, M.N. Hall, X. Liu, J. Oka, K.N. Harper, V. Slavkovich, V. Ilievski, D. Levy, A. van Geen, J.L. Mey, S. Alam, A.B. Siddique, F. Parvez, J. H. Graziano, M.V. Gamble, Blood glutathione redox status and global methylation of peripheral blood mononuclear cell DNA in Bangladeshi adults, Epigenetics 8 (2013) 728–730.
[22] I. Campesi, C. Carru, A. Zinellu, S. Occhioni, M. Sanna, M. Palermo, G. Tonolo, G. Mercuro, F. Franconi, Regular cigarette smoking influences the transsulfuration pathway, endothelial function, and inflammation biomarkers in a sex-gender specific manner in healthy young humans, Am. J. Transl. Res. 5 (2013) 497–509.
[23] G.R. Wasson, A.P. McGlynn, H. McNulty, S.L. O'Reilly, V.J. McKelvey-Martin, G. McKerr, J.J. Strain, J. Scott, C.S. Downes, Global DNA and p53 region-specific hypomethylation in human colonic cells is induced by folate depletion andreversed by folate supplementation, J. Nutr. 136 (2006) 2748–2753.
[24] K. Blaschke, K.T. Ebata, M.M. Karimi, J.A. Zepeda-Martínez, P. Goyal, S. Mahapatra, A. Tam, D.J. Laird, M. Hirst, A. Rao, M.C. Lorincz, M. Ramalho-Santos, Vitamin C induces Tet-dependent DNA demethylation and a blastocyst-like state in ES cells, Nature 500 (2013) 222–226.
[25] S. Mulero-Navarro, M. Esteller, Epigenetic biomarkers for human cancer: the time is now, Crit. Rev. Oncol. Hematol. 68 (2008) 1–11.
[26] J. Tost, DNA methylation: an introduction to the biology and the disease-associated changes of a promising biomarker, Mol. Biotechnol. 44 (2010) 71–81.
[27] S.K. Ooi, T.H. Bestor, The colorful history of active DNA demethylation, Cell 133 (2008) 1145–1148.
[28] V. Valinluck, L.C. Sowers, Endogenous cytosine damage products alter the site selectivity of human DNA maintenance methyltransferases DNMT1, Cancer Res 67 (2007) 946–950.
[29] S.M. Oba-Shinjo, M. Correa, T.I. Ricca, F. Molognoni, M.A. Pinhal, I.A. Neves, S. K. Marie, L.O. Sampaio, H.B. Nader, R. Chammas, M.G. Jasiulionis, Melanocyte transformation associated with substrate adhesion impediment, Neoplasia 8 (2006) 231–241.
[30] K.D. Robertson, E. Uzvolgyi, G. LIang, C. Talmadge, J. Sumegi, F.A. Gonzales, et al., The human DNA methyltransferases (DNMTs) 1, 3a and 3b: coordinate mRNA expression in normal tissues and overexpression in tumors, Nucleic Acids Res 27 (1999) 2291–2298.
[31] Y.A. Wang, Y. Kamarova, K.C. Shen, Z. Jiang, M.J. Hahn, Y. Wang, et al., DNA methyltransferase-3a interacts with p53 and represses p53-mediated gene expression, Cancer Biol. Ther. 4 (2005) 1138–1143.
[32] A.R. MacLeod, J. Rouleau, M. Szyf, Regulation of DNA methylation by the Ras signaling pathway, J. Biol. Chem. 270 (1995) 11327–11337.
[33] S.M. Frisch, E. Ruoslahti, Integrins and anoikis, Curr. Opin. Cell Biol. 9 (1997) 701–706.
[34] T.A. Lehman, R. Modali, P. Boukamp, p53 mutations in human immortalized epithelial cell lines, Carcinogenesis 14 (1993) 833–839.
[35] U. Henseleit, J. Zhang, R. Wanner, I. Haase, G. Kolde, T. Rosenbach, Role of p53 in UVB-induced apoptosis in human HaCaT keratinocytes, J. Invest. Dermatol. 109 (1997) 722–727.
[36] J.L. Martindale, N.J. Holbrook, Cellular response to oxidative stress: signaling for suicide and survival, J. Cell. Physiol. 192 (2012) 1–15.
[37] P. Chiarugi, From anchorage dependent proliferation to survival: lessons from redox signalling, IUBMB Life 60 (2008) 301–307.
[38] Z.T. Schafer, A.R. Grassian, L. Song, Z. Jiang, Z. Gerhart-Hines, H.Y. Irie, S. Gao, P. Puigserver, J.S. Brugge, Antioxidant and oncogene rescue of metabolic defects caused by loss of matrix attachment, Nature 461 (2009) 109–113.
[39] E. Giannoni, F. Buricchi, G. Grimaldi, M. Parri, F. Cialdai, M.L. Taddei, G. Raugei, G. Ramponi, P. Chiarugi, Redox regulation of anoikis: reactive oxygen species as essential mediators of cell survival, Cell. Death Differ. 15 (2008) 867–878.